THE JOURNAL OF PHYSICAL CHEMISTRY C

Article

pubs.acs.org/JPCC

Local Optical Activity in Achiral Two-Dimensional Gold Nanostructures

Shun Hashiyada, Tetsuya Narushima, and Hiromi Okamoto*

Institute for Molecular Science and The Graduate University for Advanced Studies (Sokendai), 38 Nishigonaka, Myodaiji, Okazaki, Aichi 444-8585, Japan

Supporting Information

ABSTRACT: Since Pasteur's discovery of molecular chirality, which means that the molecule has a nonsuperposable mirror image, the geometrical chirality of a material has been considered the prerequisite for exhibiting circular dichroism (CD, defined as the differential absorption of left and right circularly polarized light) of the structural origin. Here, we report an experimental demonstration of nanoscale local CD activities for achiral (nonchiral) rectangular gold nanostructures. Macroscopic CD spectral measurements of the nanostructure sample did not show any CD activity over the entire range of measured wavelengths, as expected from the achiral shape of the rectangle. In contrast, we found both locally positive and negative CD signals in a single rectangular nanostructure, whose distribution was symmetric about the center of the rectangle, with large CD signals at the corners. The results demonstrate that the established selection rule of optical activity is not valid for local microscopic measurements.

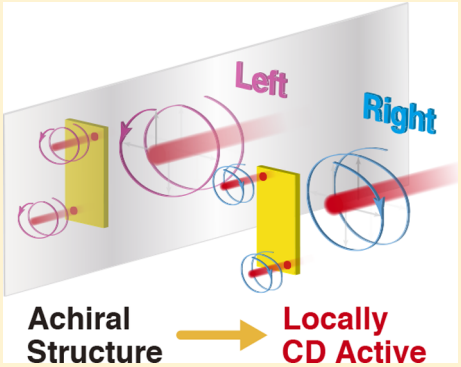

INTRODUCTION

Many molecules such as amino acids and sugars possess chirality, i.e., the molecule is not superposable onto its mirror image. The optical response of such a chiral molecule to circularly polarized light (CPL), depending on its handedness, is known as the optical activity.[1] Circular dichroism (CD), which is defined as the differential absorption of left and right CPL, provides a measure of optical activity. In macroscopic optical measurements, chiral molecules generally show CD activity, whereas achiral (nonchiral) molecules do not. Since Pasteur's discovery of molecular chirality, the structural chirality in a material is considered the prerequisite for exhibiting CD activity of the structural origin, as described in many representative textbooks.[1−3]

Recently, macroscopic CD activity of two-dimensional (2D) metallic nanostructures with chiral shapes was reported,[4−7] and the observed CD signal was several orders of magnitude greater than those arising from typical chiral molecules.[6] In contrast, achiral 2D nanostructures did not show any macroscopic CD activity when the light incidence was normal to the nanostructure sample surface.[6] However, when the achiral 2D structure was anisotropic, it showed the macroscopic CD activity under off-normal incidence of light even without structural chirality in the material.[8−10] In this case, a mutual arrangement of the incident light and the nanostructure material produced the chirality, which caused the CD activity to emerge.

According to a recent report, chiral metal nanostructures not only show significant macroscopic CD activity but also enhance the optical activity signals from chiral molecules near the nanostructures by several orders of magnitude.[11] Some theoretical studies noted that the interaction between the chiral nanostructures and light could generate highly twisted optical fields near the nanostructures.[12,13] The twisted optical fields, as typified by CPL, correspond to electromagnetic fields with nonzero optical chirality.[14,15] Highly twisted optical fields, which have larger optical chiralities than ordinary CPL, can be generated under special circumstances.[12,13] It was also theoretically shown that a metal nanosphere could enhance the optical chirality of CPL in its periphery.[16]

To fully understand and control the optical activity of nanostructures and the highly twisted optical fields, it is crucial to obtain direct information on the local CD activity in the nanostructures. In our previous work, we compared the experimentally obtained macroscopic and local CD activities of 2D chiral gold nanostructures.[17] The nanoscale CD imaging measurements at the spectral peak wavelength of the material revealed both positive and negative CD signals in the individual nanostructure, and the local CD signal was much (2 orders of magnitude) larger than the macroscopic CD signal. It was speculated that only a tiny CD signal remained after averaging over the entire system because the local CD signals with alternating signs were distributed over the nanostructure.

Recently, it was theoretically predicted that upon the irradiation of linearly polarized light, twisted optical fields are locally generated near slab-like metal nanostructures with

Received: July 18, 2014
Revised: August 21, 2014
Published: August 26, 2014

   dx.doi.org/10.1021/jp507168a | J. Phys. Chem. C 2014, 118, 22229−22233

achiral symmetries.[18,19] Although the chirality of a material is the prerequisite for macroscopic CD activity, these theoretical studies suggest that the achiral nanostructures can yield local CD activity. In the present study, we perform a near-field CD (NF-CD) imaging study for 2D achiral gold nanostructures to explore the local CD activities. We also discuss the possible origins of the local CD features and the correlation between the local CD activity and the structural chirality using an electromagnetic field simulation.

EXPERIMENTAL SECTION

Optimized Design of Achiral Nanostructured Sample. We chose a gold rectangle as a highly symmetric achiral 2D nanostructure. The nanostructure was fabricated on a glass substrate using the electron-beam lithography lift-off technique. The measured dimensions of the fabricated rectangle were 310 nm long and 170 nm wide. A gold film with a thickness of 50 nm was formed by vacuum deposition onto an underlying 2 nm thick chromium adhesion layer. Two types of samples that consist of rectangular gold nanostructures were prepared as follows. One type is prepared for the macroscopic spectral measurements. A high areal density of the metal nanostructures was necessary to determine the macroscopic optical property of the rectangle with sufficient accuracy. Thus, we prepared a sample with a total area of 400 × 400 μm^2 and rectangles at intervals of approximately 700 nm. The fabricated rectangles covered 5.3% of the entire area of the arrayed sample substrate. The other sample is for near-field optical measurements. In this case, diffraction and scattering by neighboring nanostructures should be negligible. Thus, the interval between rectangles in the sample was approximately 1600 nm, which was much larger than that in the sample for the macroscopic measurements, and the areal density of the nanostructures was 1.1%. The individual rectangular structure has a 2-fold rotational symmetry in the 2D plane. Because of the inherent properties of the CD measurement, which was equipped with a photoelastic modulator (PEM), the commingling of linear dichroism (LD), which occurs because of the anisotropy of the rectangle, in the CD signals is anticipated. The experimental details of cancellation of LD contributions to macroscopic and local CD measurements are described in the Supporting Information.

Macroscopic Optical Measurements. Macroscopic optical extinction spectra (here, extinction includes contributions from absorption and scattering) were measured using a standard far-field optical microscope, and the CD spectra were obtained using a conventional CD spectrometer (J-720WI, JASCO Corp.), which is equipped with a PEM. To measure the extinction spectra, white light from a xenon discharge arc lamp was focused onto the arrayed nanostructure sample through an objective lens (numerical aperture (NA) = 0.7). The transmitted light caused by absorption and scattering was collected using another objective lens (NA = 0.8) and detected using a fiber-optic spectrometer to acquire the extinction spectra. For the CD measurements, the light for detection was illuminated onto the sample as a parallel beam that was normal to the sample surface with a large diameter (~8 mm). Because the arrayed nanostructure sample, which was fabricated with an area of 400 × 400 μm^2, occupies only a notably small areal fraction of the large-diameter incident beam (400 × 400 μm^2 of ~50 mm^2), it was difficult to obtain sufficient signal levels. Thus, we spatially restricted the size of the parallel light beam with an aperture (400 μm in diameter) to increase the fraction of light that illuminated the metal nanostructures relative to the total incident flux. This treatment improved the sensitivity of the CD signal from the nanostructure sample.

Near-Field Optical Measurements. To visualize the distribution of the local CD signals in the individual nanostructures, we combined a collection-mode aperture-type scanning near-field optical microscope with a polarization modulation method using a PEM.[20] The modulated light was normally incident onto the sample substrate. The aperture diameter of the near-field probes was typically 50−100 nm, which also gives the approximate spatial resolution of the NF-CD imaging.

Definition of CD Signals. In this report, $\Delta A = A_{LCP} - A_{RCP}$ defines the CD signal, where A_{LCP} and A_{RCP} denote the absorbance ($A = \log_{10}(I_0/I)$ where I and I_0 denote transmission intensities at the sample and at the bare substrate, respectively; A includes contributions from absorption and scattering) for left and right CPL, respectively. From the definition, $\Delta A > 0$ when the left CPL has a higher extinction than the right CPL. The quantity ΔA can be converted to the ellipticity θ, which is frequently used for the CD activity of molecules, using the relation $\theta(\mathrm{deg}) = 32.982\Delta A$ when ΔA is sufficiently small.[2]

RESULTS

Figure 1a,b shows the macroscopic extinction and the CD spectra, respectively, of the arrayed rectangular gold nanostructure sample. The vertical axes in Figure 1a,b (absorbance and ΔA, respectively) were corrected for the factor of the relative areal fraction (5.3%). The extinction spectrum exhibited a broad band because of plasmon resonances with a peak at approximately 900 nm. The CD spectrum did not show any

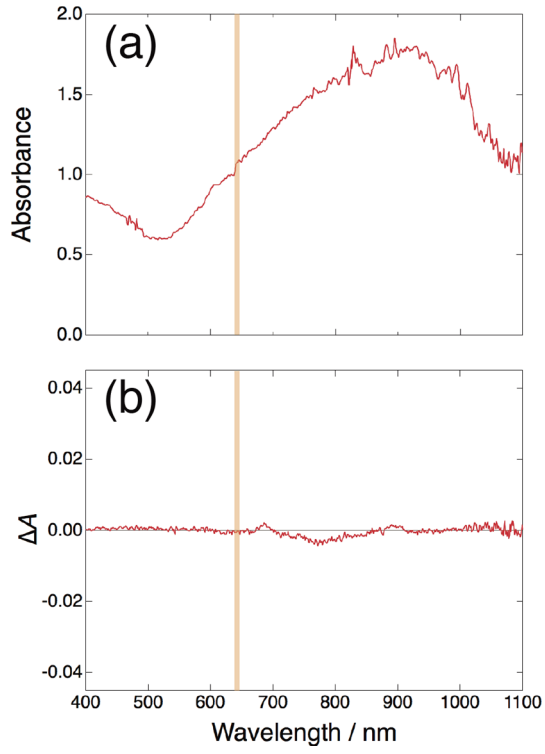

Figure 1. Macroscopic extinction (a) and CD (b) spectra of the arrayed rectangular gold nanostructures. The excitation wavelength (633 nm) used for the NF-CD imaging is indicated by the vertical lines.

dx.doi.org/10.1021/jp507168a | J. Phys. Chem. C 2014, 118, 22229−22233

distinct signal over the entire range of measured wavelengths. The small fluctuation of the CD signal is within a negligible level, considering the CD signals found for achiral metal nanostructures in the preceding work,[6] and may be attributed to imperfect geometry of the nanostructures. This result indicates that the entire system of the rectangular gold nanostructures is not optically active, as expected from the achiral structure.

In contrast, we observed locally strong CD signals when the CD measurement is spatially resolved on the rectangle. The chosen wavelength for the near-field optical measurements was 633 nm, where a plasmon resonance can be excited on the nanostructures, as observed in Figure 1a, whereas the macroscopic CD signal was negligible ($|\Delta A| < 10^{-3}$) at this wavelength (Figure 1b). Figure 2a,2b shows the near-field

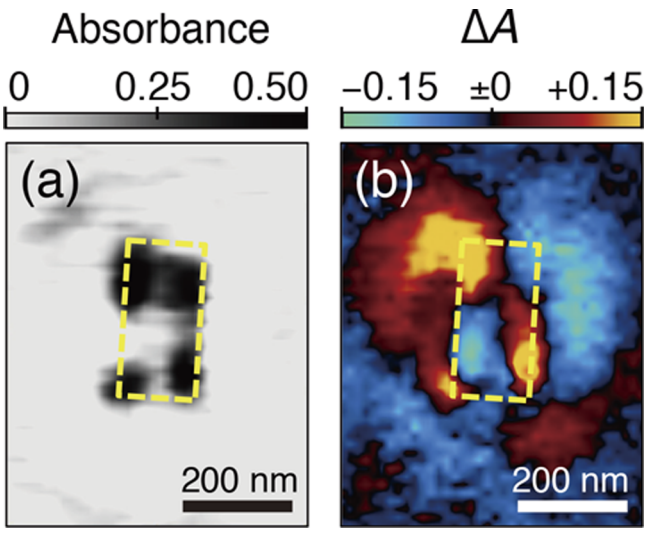

Figure 2. Near-field optical images of a gold nanorectangle. Simultaneously obtained near-field extinction (a) and NF-CD (b) images for a single rectangular gold nanostructure. The observation wavelength was 633 nm. The dashed lines indicate the position of the gold rectangle.

extinction and the CD images, respectively, for a single gold rectangle, which were simultaneously obtained using the near-field imaging system. In the near-field extinction image (Figure 2a), strong extinction was observed near the four corners of the rectangle. The localized extinction at the corners is evidence of the plasmon-mode excitation. In the simultaneously obtained NF-CD image (Figure 2b), the extremal values of local CD signals were observed at these corners. The local CD signals showed a point-symmetric (or 2-fold rotationally symmetric) distribution about the center of the rectangle, which correctly reflected the structural symmetry of the nanostructure. The extremal CD signals had the same sign at the diagonal corners and opposite signs at the adjacent ones. Within the experimental uncertainty, the local CD signals symmetrically arranged for any orientation angle of the rectangle, which confirms that the observed CD signal distribution arose from an intrinsic origin of the nanostructures instead of artifacts such as LD (see Supporting Information). The symmetric distribution of the positive and negative CD signals in the individual rectangular nanostructure leads to approximately null CD activity on average over the entire rectangle. This result is consistent with the macroscopically obtained CD spectrum (Figure 1b), which showed a negligibly small (essentially zero) CD signal.

The observed local CD signals of the nanostructure had much larger magnitudes than those of typical chiral molecules. Here, the CD signal that was normalized with its absorbance, $|g| = |\Delta A/A|$, is a parameter to compare the CD activities of different materials. For the rectangular gold nanostructures, the CD signal amplitudes $|\Delta A|$ and the absorbance A were ∼0.15 and ∼0.5, respectively, at the corners; consequently, $|g|$ is estimated to be ∼0.3. For a typical chiral molecule, such as flavin mononucleotide, $|g|$ was $\sim 2.0 \times 10^{-3}$ at 450 nm.[21] We find that the local CD of the rectangular nanostructure was 2 orders of magnitude larger than the CD signal of the typical chiral molecule, although it did not show any CD activity macroscopically. Thus, strong CD activity at local regions of achiral nanostructures has been experimentally proven in our study.

DISCUSSION

The observed circular dichroism of the achiral rectangular gold nanostructure apparently violates the established selection rule of optical activity. However, although locally strong CD was observed, the macroscopic CD was null for this rectangle, and the results were logically consistent with the conventional rule of optical activity. The relevant phenomenon, i.e., the generation of twisted optical fields near the metal slab structures, was theoretically discussed based on the electromagnetic field simulation in the preceding study.[18,19] Here, we qualitatively explain the observed local CD activity in the rectangle. Suppose that the rectangle is irradiated by right CPL. If we assume that the electric field (or the induced polarization) at corner A (Figure 3a) is in the direction of the short side at a certain moment, then after a quarter period, the field (or the polarization) will be in the direction of the long side. The situation is exactly identical for the opposite corner A′. The

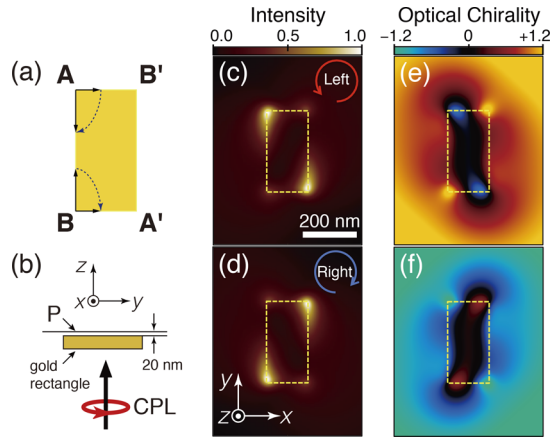

Figure 3. Model analysis for the local CD of the nanorectangle. (a) Time evolution of the induced polarization at the corners upon right CPL irradiation. (b) The model of the FDTD simulation. The electromagnetic fields were evaluated at the plane indicated by "P". Steady state distributions of (c,d) electromagnetic-field intensity and (e,f) optical chirality for the rectangular gold nanostructure were simulated under CPL illumination at 633 nm; (c,e) left CPL and (d,f) right CPL. The simulated electromagnetic-field intensity was normalized by the maximum intensity for each panel. The optical chirality was normalized by that of left CPL (i.e., left CPL corresponds to +1 and right CPL to −1).

dx.doi.org/10.1021/jp507168a | J. Phys. Chem. C 2014, 118, 22229−22233

induced-polarization magnitude depends on the polarization direction, i.e., the induced polarizations along the long-side direction, short-side direction, inner direction, and outer direction are generally all different from each other. At corners B and B′, the field and the polarization are first in the long-side direction; after a quarter period, they changed to the short-side direction. In other words, the polarization transitions occur in reversed order from those at corner A. In this situation, the optical response to CPL at corners A and B are different from each other if the system behavior is irreversible because of the energy dissipation after the plasmon excitation. The response to left CPL should be reversed from that described above for right CPL. Thus, we qualitatively understand that the rectangle shows optical activity near the corners, and the spatial distribution of the optical activity signal reflects the structure symmetry.

We performed a three-dimensional electromagnetic simulation using the finite-difference time-domain (FDTD) method for the presently studied nanostructures to discuss the mechanism of the local CD activity. The FDTD simulations were conducted using a commercial software program (Poynting for Optics, Fujitsu, Japan). The simulation box size was 1000 nm × 1000 nm × 1000 nm in x, y, and z directions, and the perfect matching layer boundary condition was adopted. The simulated metal nanostructure had identical dimensions as those in the experiments. The rectangular nanostructure was excited by plane wave at 633 nm to simulate the condition for the NF-CD measurement. The configuration of the incident light and the nanostructure is shown in Figure 3b. The electromagnetic field was evaluated at a plane 20 nm above the top surface of the gold nanostructure to mimic the separation between the sample and the near-field probe. Figure 3c–f show the simulated steady state distributions of electromagnetic field intensity (Figure 3c,d) and optical chirality (Figure 3e,f) of the rectangular nanostructure under illuminations of left and right CPL, respectively. Enhanced optical fields are located at corners A and A′ under the left CPL illumination, whereas the enhanced fields are at corners B and B′ under the right CPL illumination. This simulated result demonstrates that the CPL illumination onto the rectangular nanostructure yields an electromagnetic-field distribution with a spatial symmetry lower than the symmetry of the rectangle. Thus, the local CD activities may be attributed to the difference in optical responses to left and right CPL at the rectangle corners. The enhanced optical fields were distributed around the corners in the computed results in Figure 3c,d, which indicates that the electromagnetic local densities of states (LDOS) are strengthened at these sites. The local transmission is sometimes effectively suppressed where the LDOS is high (whether the transmitted light is suppressed or enhanced depends on the resonance condition of the observation).[22,23] Considering this effect, the simulated spatial features of electromagnetic fields under the CPL illumination qualitatively explain the strong local extinction (Figure 2a) and the local CD (Figure 2b) around the corners, which were experimentally observed for the rectangular gold nanostructure. The result suggests that a chiral shape of the nanostructures is not a prerequisite for local CD activity. Instead, the chiral distribution of the electromagnetic field, which is caused by the interaction of light with the matter, is indispensable. Currently, the type of plasmon modes that generate the chiral optical field has not been clarified. This issue will be solved using systematic investigations on the dependences of the local CD activity on the excitation wavelength, the size, and the dimensions of the nanostructures. We should also note that the present simulation did not directly model the experimental near-field observation because the observing system (in particular, the near-field probe) was not considered in the simulation. In future works, the observation system should be incorporated in the theoretical analysis for further understanding.

CONCLUSIONS

In this study, the local CD activity in 2D achiral rectangular gold nanostructures was directly observed using an NF-CD imaging system. We experimentally demonstrated that the rectangular gold nanostructure showed locally strong CD activity (2 orders of magnitude greater than the CD of typical chiral molecules) at the corners, although it showed no CD activity macroscopically. The averaged local CD signal over the entire nanostructure was approximately zero because the CD signal was symmetrically distributed, which is consistent with the macroscopic null CD activity. We simulated the electromagnetic field distribution near the nanostructure based on the FDTD method and found that the CPL illumination forms a chiral distribution of optical fields. The generated chiral optical-field distribution is considered the origin of the local CD activity for achiral nanostructures. In conclusion, the chirality of a material is essential in the macroscopic CD activity of 2D nanostructures when the light incidence is normal to the nanostructure sample surface, but the structural chirality of the nanostructure is not essential for local CD activity. Instead, the chirality (or asymmetry) of optical-field distribution that is produced by the interaction of circularly polarized light with the material is crucial. The present result provides the indispensable basis for discussion of spectrochemical and microscopic analyses of the optical activity of nanostructured materials and molecules.

ASSOCIATED CONTENT

Supporting Information

Detailed information for cancellation of linear dichroism contribution and additional figures. This material is available free of charge via the Internet at http://pubs.acs.org.

AUTHOR INFORMATION

Corresponding Author

*(H.O.) E-mail: aho@ims.ac.jp. Fax: +81-564-54-2254. Tel: +81-564-55-7320.

Notes

The authors declare no competing financial interest.

ACKNOWLEDGMENTS

The authors thank Ms. A. Ishikawa (IMS) for the nanostructure sample fabrication and Mr. S. Makita (IMS) for his help with the macroscopic CD measurements. This work was supported by Grants-in-Aid for Scientific Research (Grant Nos. 21655008, 22225002, and 23760038) from the Japan Society for the Promotion of Science.

REFERENCES

(1) Barron, L. D. *Molecular Light Scattering and Optical Activity*, 2nd ed.; Cambridge Univ. Press: Cambridge, U.K., 2004.

(2) Berova, N.; Nakanishi, K.; Woody, R. W. *Circular Dichroism: Principles and Applications*, 2nd ed.; Wiley-VCH: New York, 2000.

(3) Atkins, P. W.; de Paula, J. *Physical Chemistry*, 10th ed.; Oxford Univ. Press: Oxford, U.K., 2014.

(4) Papakosatas, A.; Potts, A.; Bangnall, D. M.; Provirnin, S. L.; Coles, H. J.; Zheludev, N. I. Optical Manifestations of Planar Chirality. *Phys. Rev. Lett.* **2003**, *90*, 107404.
(5) Vallius, T.; Jefimovs, K.; Turunen, J.; Vahimaa, P.; Svirko, Y. Optical Activity in Subwavelength-Period Arrays of Chiral Metallic Particles. *Appl. Phys. Lett.* **2003**, *83*, 234−236.
(6) Kuwata-Gonokami, M.; Saito, N.; Ino, Y.; Kauranen, M.; Jefimovs, K.; Vallius, T.; Turunen, J.; Svirko, Y. Giant Optical Activity in Quasi-Two-Dimensional Planar Nanostructures. *Phys. Rev. Lett.* **2005**, *95*, 227401.
(7) Drezet, A.; Genet, C.; Laluet, J. Y.; Ebbesen, T. W. Optical Chirality without Optical Activity: How Surface Plasmons Give a Twist to Light. *Opt. Express* **2008**, *16*, 12559−12570.
(8) Plum, E.; Fedotov, V. A.; Zheludev, N. I. Optical Activity in Extrinsically Chiral Metamaterial. *Appl. Phys. Lett.* **2008**, *93*, 191911.
(9) Plum, E.; Liu, X.-X.; Fedotov, V. A.; Chen, Y.; Tsai, D. P.; Zheludev, N. I. Metamaterials: Optical Activity without Chirality. *Phys. Rev. Lett.* **2009**, *102*, 113902.
(10) Yannopapas, V. Circular Dichroism in Planar Nonchiral Plasmonic Metamaterials. *Opt. Lett.* **2009**, *34*, 632−634.
(11) Hendry, E.; Carpy, T.; Johnston, J.; Popland, M.; Mikhaylovskiy, R. V.; Lapthorn, A. J.; Kelly, S. M.; Barron, L. D.; Gadegaard, N.; Kadodwala, M. Ultrasensitive Detection and Characterization of Biomolecules Using Superchiral Fields. *Nat. Nanotechnol.* **2010**, *5*, 783−787.
(12) Hendry, E.; Mikhaylovskiy, R. V.; Barron, L. D.; Kadodwala, M.; Davis, T. J. Chiral Electromagnetic Fields Generated by Arrays of Nanoslits. *Nano Lett.* **2012**, *12*, 3640−3644.
(13) Schäferling, M.; Dregely, D.; Hentschel, M.; Giessen, H. Tailoring Enhanced Optical Chirality: Design Principles for Chiral Plasmonic Nanostructures. *Phys. Rev. X* **2012**, *2*, 031010.
(14) Tang, Y.; Cohen, A. E. Optical Chirality and Its Interaction with Matter. *Phys. Rev. Lett.* **2010**, *104*, 163901.
(15) Choi, J. S.; Cho, M. Limitations of a Superchiral Field. *Phys. Rev. A* **2012**, *86*, 063834.
(16) García-Etxarri, A.; Dionne, J. A. Surface-Enhanced Circular Dichroism Spectroscopy Mediated by Nonchiral Nanoantennas. *Phys. Rev. B* **2013**, *87*, 235409.
(17) Narushima, T.; Okamoto, H. Strong Nanoscale Optical Activity Localized in Two-Dimensional Chiral Metal Nanostructures. *J. Phys. Chem. C* **2013**, *117*, 23964−23969.
(18) Schäferling, M.; Yin, X.; Giessen, H. Formation of Chiral Fields in a Symmetric Environment. *Opt. Express* **2012**, *20*, 26326−26336.
(19) Davis, T. J.; Hendry, E. Superchiral Electromagnetic Fields Created by Surface Plasmons in Nonchiral Metallic Nanostructures. *Phys. Rev. B* **2013**, *87*, 085405.
(20) Narushima, T.; Okamoto, H. Circular Dichroism Nano-Imaging of Two-Dimensional Chiral Metal Nanostructures. *Phys. Chem. Chem. Phys.* **2013**, *15*, 13805−13809.
(21) Abdulrahman, N. A.; Fan, Z.; Tonooka, T.; Kelly, S. M.; Gadegaard, N.; Hendry, E.; Govorov, A. O.; Kadodwala, M. Induced Chirality Though Electromagnetic Coupling Between Chiral Molecular Layers and Plasmonic Nanostructures. *Nano Lett.* **2012**, *12*, 977−983.
(22) Shimada, T.; Imura, K.; Hossain, M. K.; Okamoto, H.; Kitajima, M. Near-Field Study on Correlation of Localized Electric Field and Nanostructures in Monolayer Assembly of Gold Nanoparticles. *J. Phys. Chem. C* **2008**, *112*, 4033−4035.
(23) Harada, Y.; Imura, K.; Okamoto, H.; Nishijima, Y.; Ueno, K.; Misawa, H. Plasmon-Induced Local Photocurrent Changes in GaAs Photovoltaic Cells Modified with Gold Nanospheres: A Near-Field Imaging Study. *J. Appl. Phys.* **2011**, *110*, 104306.